DOI: 10.5516/NET.2011.43.1.025

FIRST ATLAS DOMESTIC STANDARD PROBLEM (DSP-01) FOR THE CODE ASSESSMENT

YEON-SIK KIM*, KI-YONG CHOI, KYOUNG-HO KANG, HYUN-SIK PARK, SEOK CHO, WON-PIL BAEK, KYUNG-DOO KIM, SUK K. SIM[1], EO-HWAK LEE[2], SEYUN KIM[3], JOO-SUNG KIM[4], TONG-SOO CHOI[5], CHEOL-WOO KIM[6], SUK-HO LEE[7], SANG-IL LEE[8], and KEO-HYOUNG LEE[9]
Thermal Hydraulics Safety Research Division,
Korea Atomic Energy Research Institute
1045 Daedeokdaero, Yuseong-gu, Daejeon 305-353, Rep. of Korea
[1]EN2T, [2]KAIST, [3]KEPRI, [4]KINS, [5]KNF, [6]KOPEC, [7]NETEC, [8]SDD, [9]SNU
*Corresponding author. E-mail : yskim3@kaeri.re.kr

Received October 28, 2010
Accepted for Publication December 24, 2010

KAERI has been operating an integral effect test facility, ATLAS (Advanced Thermal-Hydraulic Test Loop for Accident Simulation), for accident simulations of advanced PWRs. Regarding integral effect tests, a database for major design basis accidents has been accumulated and a Domestic Standard Problem (DSP) exercise using the ATLAS has been proposed and successfully performed. The ATLAS DSP aims at the effective utilization of an integral effect database obtained from the ATLAS, the establishment of a cooperative framework in the domestic nuclear industry, better understanding of thermal hydraulic phenomena, and an investigation of the potential limitations of the existing best-estimate safety analysis codes. For the first ATLAS DSP exercise (DSP-01), integral effect test data for a 100% DVI line break accident of the APR1400 was selected by considering its technical importance and by incorporating comments from participants. Twelve domestic organizations joined in this DSP-01 exercise. Finally, ten of these organizations submitted their calculation results. This ATLAS DSP-01 exercise progressed as an open calculation; the integral effect test data was delivered to the participants prior to the code calculations. The MARS-KS was favored by most participants but the RELAP5/MOD3.3 code was also used by a few participants. This paper presents all the information of the DSP-01 exercise as well as the comparison results between the calculations and the test data. Lessons learned from the first DSP-01 are presented and recommendations for code users as well as for developers are suggested.

KEYWORDS : ATLAS, Integral Effect Test, DVI, SBLOCA, Thermal-Hydraulic, DSP

1. INTRODUCTION

KAERI (Korea Atomic Energy Research Institute) has been operating an integral effect test facility, ATLAS (Advanced Thermal-Hydraulic Test Loop for Accident Simulation), for accident simulations for the OPR1000 (Optimized Power Reactor, 1000MWe) and the APR1400 (Advanced Power Reactor, 1400MWe), which are in operation and under construction, respectively, in Korea [1~4].

In 2007, the ATLAS was extensively used for a broad range of the integral effect tests on the reflood phase of a large break LOCA (LBLOCA) in order to resolve safety issues of the APR1400 that were raised by a regulatory organization during its licensing process for design certification. The ATLAS was modified afterwards to have a configuration for simulating the direct vessel injection (DVI) line break accidents of the APR1400 at the beginning of 2008. Sensitivity tests for different DVI line break sizes were performed in 2008 [5]. Integral effect databases for four break sizes were established; 5%, 25%, 50%, and 100%. The ATLAS has been used to provide the unique integral effect test data for the 2 (hot legs) $\times$ 4 (cold legs) reactor coolant system (RCS) with a DVI of the emergency core cooling (ECC) water; this will significantly expand the currently available data bases for the code validation.

1.1 Background and Brief History

A Domestic Standard Problem (DSP) exercise using the ATLAS was proposed and discussed at the MARS (Multi-dimensional Analysis of Reactor Safety) user group meeting and the 3rd Nuclear Safety Analysis Symposium in 2005. The discussion at the symposium (with potential

domestic participants) revealed that the ATLAS DSP would contribute to improving the safety analysis methodology for pressurized water reactors (PWRs). Since then, KAERI has prepared an "ATLAS DSP Research Agreement" document taking into account the potential participants' opinions and dispatched it in 2006. Eventually, fourteen domestic organizations had approved the agreement by April, 2008.

An ATLAS DSP kick-off meeting was held together with the CAMP/MUG (Code Assessment and Maintenance Program/MARS User Group) meeting in June, 2008. At that meeting, KAERI presented preliminary test results for a 25% DVI line break of the APR1400 and proposed it as a potential candidate for an ATLAS DSP exercise. Most participants expressed positive opinions that the ATLAS DSP would be beneficial and helpful for the safety analysis research. After the kick-off meeting, a total of four progress meetings were held from June, 2009 to February, 2010. In the first progress meeting, the 100% DVI line break test (SB-DVI-08 test) was selected as the ATLAS DSP-01 exercise because the 100% DVI line break case has more technical importance and is of more phenomenological interest than the 25% DVI line break case. Further details on the progress meetings can be found in reference 6.

The final workshop was held in April, 2010 at KAERI. Ten domestic organizations presented their final calculation results, followed by an in-depth technical discussion on the major outcome of the present DSP-01 exercise. The water levels of the core and the downcomer regions, the ECC bypass rate, the multi-dimensional phenomena in the downcomer, the loop seal clearing phenomena, and the loop flow characteristics were, especially, identified as the crucial phenomena for closer investigation from the viewpoint of code modeling.

1.2 Objectives of the ATLAS DSP-01

A best-estimate safety analysis methodology for small break LOCAs including the DVI line break needs to be developed to identify the uncertainties involved in the present safety analysis results, which are based on the conservative evaluation models. Such a best-estimate safety analysis methodology will contribute to defining a more precise specification of a safety margin and thus will provide greater flexibility to regulators and operators as well. However, such an effort has not been realized yet because of the lack of an integral effect test database.

The objectives of the present DSP-01 exercise can be summarized as follows:

- Effective utilization of the integral effect database obtained from the ATLAS.
- Establishment of a cooperative framework among the domestic nuclear industries, academic institutes, and research and regulation organizations.
- Better understanding of thermal-hydraulic phenomena in the upper annulus downcomer during the DVI injection period of SBLOCAs.
- Investigation of the potential limitations of the existing best-estimate safety analysis codes and suggestion of physical phenomena for further code improvements.
- Characterization of the user effect of the best-estimate codes.

1.3 Organization of the ATLAS DSP-01

The ATLAS DSP-01 was led by KAERI in collaboration with KINS. KAERI was responsible for the general coordination of the DSP-01, which includes supplying the experimental data and information on the ATLAS facility, performing an independent code calculation, integrating calculation results, organizing progress meetings and a final workshop, and preparing a final comparison report. As a joint operating agency, KINS was responsible for providing support to the general coordination of KAERI and performing a code calculation as one of the participants.

Twelve organizations joined the ATLAS DSP-01 program as listed in Table 1. Each (signed) organization had an obligation to perform an open calculation on a certain due date with the test data provided by the host organization, KAERI. All the participants were also requested to write their analysis results in their assigned section of the comparison report [6]. Unfortunately, two organizations did not manage to finish their calculations due to a shortage of manpower, as shown in Table 1.

2. THE ATLAS FACILITY AND TEST DESCRIPTION

2.1 Overview of the ATLAS

The ATLAS is a large-scale thermal-hydraulic integral effect test facility for advanced PWRs, APR1400 and OPR1000. It can simulate a wide range of the accident and transient conditions including large- and small-break LOCAs. The information on the ATLAS program, major design characteristics, scoping analyses, commissioning test results, and some major test results can be found in the literature [5,7,8~11]. Fig. 1 shows a flow diagram of the ATLAS facility for the 100% DVI line break test.

2.2 Experimental Condition and Procedure of the SB-DVI-08 Test

The 100% DVI line break test of the ATLAS, named the SB-DVI-08, was performed according to the following experimental procedure. Basically, the experimental conditions for the present test were determined by a pre-test calculation with a best-estimate thermal hydraulic code, MARS3.1. First of all, a transient calculation was performed for the DVI line break of the prototypic plant, APR1400, to obtain the reference initial and boundary conditions. A best-estimate safety analysis methodology that is now commonly accepted in the nuclear community was applied to the transient calculation of the APR1400. The safety

Table 1. List of DSP-01 Participants

No.	Participants	Code	Remarks
1	ACT	MARS-KS	Withdrawal
2	EN2T	MARS-KS	
3	Doosan Heavy Industry	MARS-KS	Withdrawal
4	KAERI	MARS-KS	DC multi-D
5	KAIST	MARS-KS	Double channel DC
6	KEPRI	MARS-KS	
7	KINS	MARS-KS	
8	KNF	RELAP5/MOD3.3	
9	KOPEC/AE	RELAP5-ME	Combined into 'KOPEC/SD'
	KOPEC/SD	RELAP5-ME	
10	NETEC	RELAP5/MOD3.3	
11	SDD	MARS-KS	
12	SNU	MARS-KS	

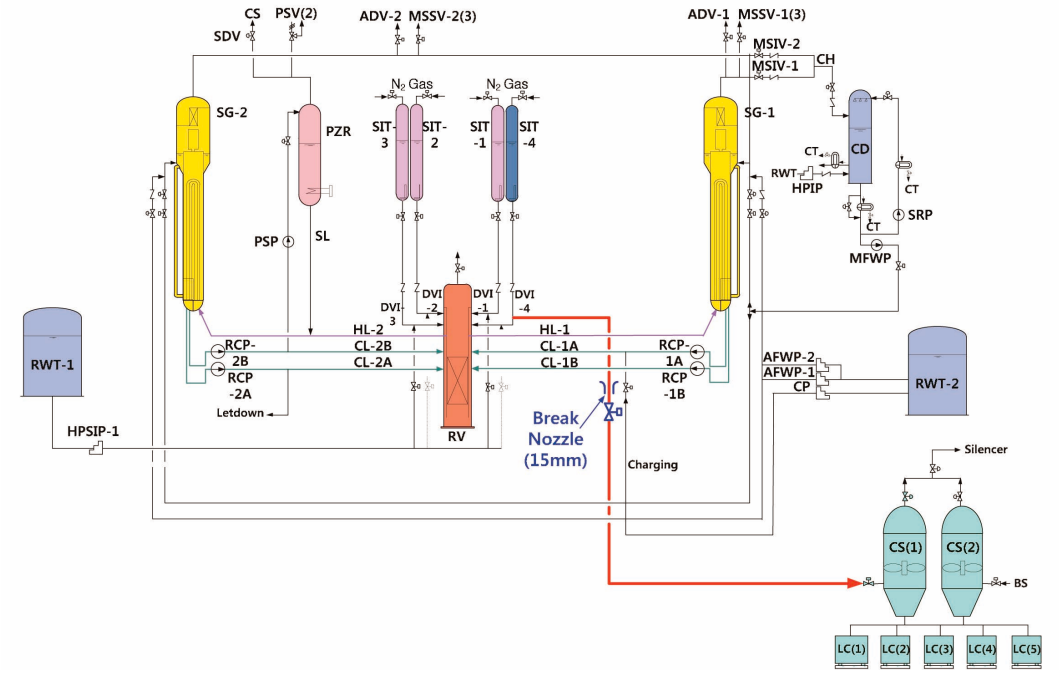

Fig. 1. Configuration of 100% DVI Line Break of the ATLAS Facility

injection system of the APR1400 has four mechanically separated hydraulic trains. They are also electrically separated by two divisions, implying that each emergency diesel generator powers two hydraulic trains. The pre-test calculation was conducted with the assumption that the loss of off-site power occurred simultaneously with the break and the limiting single failure as a loss of a diesel generator resulted in the minimum safety injection to the core.

Furthermore, the safety injection flow to the broken DVI-4 nozzle was not credited. Therefore, the safety injection flow by the safety injection pump (SIP) was injected only through the DVI-2 nozzle opposite the broken DVI-4 nozzle.

As regards the safety injection flow by the four safety injection tanks (SIT), three SITs except for the SIT connected to the broken DVI-4 nozzle were available to provide the safety injection flow into the core. As for the core power, a conservative 1973 ANS decay heat curve

with 1.2 multiplication factor was used in the transient calculation. In the DVI line break, the containment back-pressure does not affect the progression of the transient, because a choking condition is maintained throughout the transient. Therefore, the containment back-pressure was not an important control parameter in the present test.

The SB-DVI-08 test was performed at the same pressure as that of the reference plant, APR1400. The temperature distribution along the primary loop was also preserved. The primary inventory was heated with core heaters to its specified steady state condition and was pressurized by a pressurizer until the primary system reached a steady state condition. During the primary heat-up process, the secondary system was also heated up to a specified target hot condition by controlling the heat removal rate from the primary system. At a steady state condition, the core power generated by electrical heaters was balanced with the energy removal by the secondary system. The obtained steady state condition was maintained constant to stabilize the system behavior of the ATLAS for more than ten minutes.

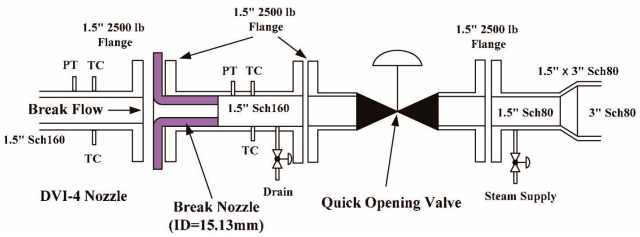

Fig. 2. Configuration of the Break Simulation System for the DVI line Break Tests

After a steady state condition in the whole ATLAS system was maintained for more than ten minutes, the transient test was commenced. The DVI line break test was initiated by opening a quick-opening break valve, OV-BS-03, at the break spool piece. A DVI line break was simulated by installing a break spool piece at one of the DVI nozzles. The configuration of the break spool piece is shown in Fig. 2. It consists of a quick opening valve, a break nozzle, a case holding the break nozzle, and a few instruments. The break nozzle was installed vertically downward at the discharge line of the DVI nozzle. The quick opening valve was opened within 0.5 seconds by operators when the test was initiated. The break flow was discharged to the containment simulating system.

When the pressurizer pressure reached a specified pressure of 10.72 MPa, the low pressurizer pressure (LPP) signal was automatically generated by embedded control logics. The heaters of the pressurizer and all tracing heaters in the primary system were tripped at the same time as the LPP signal. The reactor coolant pump (RCP) was automatically tripped with a time delay of 0.35 seconds after the LPP signal. The main steam and the main feedwater lines were isolated with a time delay of 0.1 seconds and 7.1 seconds after the LPP signal, respectively. The SIP was actuated by the LPP signal with a time delay of 28.3 seconds.

When the downcomer pressure became lower than the specified pressure of 4.03 MPa, the SIT started to deliver the safety injection flow to the reactor pressure vessel. The detailed sequence of events applied to the present test is summarized in Table 2. A summary of the initial and the boundary conditions for the present test is also shown in Table 3.

Table 2. Comparison of the Sequence of a DVI Line Break (100% Break)

Events	APR1400 (time,sec)	ATLAS (time,sec)	Description
Break open	0	0	
Low pressurizer pressure trip (LPP)	20.9		If pressurizer pressure < 10.72 MPa
Pressurizer heater trip	LPP + 0.0	LPP + 0.0	
Reactor scram & RCP trip	LPP + 0.5	LPP + 0.35	Delay time is reduced by a square root of two
Turbine isolation	LPP + 0.1	LPP + 0.07	
Main feedwater isolation	LPP + 10	LPP + 7.07	
Safety injection pump start	LPP + 40	LPP + 28.28	
Low upper downcomer pressure trip (LUDP)	LUDP	LUDP	If downcomer pressure < 4.03MPa
Safety injection tank (SIT) start	LUDP + 0.0	LUDP + 0.0	
Low flow turndown of the SIT			If water level of the SIT is less than a specified set point

Table 3. Measured Initial Conditions for a 100% DVI Line Break Test

parameter	Measured value	Instruments	Remarks
Primary system			
- Core power (MW)	1.647	-	Including heat loss
- Heat loss (kW)	88/57	Primary/Secondary	Estimation
- PZR Pressure (MPa)	15.49	PT-PZR-01	Pressurizer
- Core inlet temp. (K)	563.2	TF-LP-02G18	
- Core exit temp.(K)	598.9	TF-CO-07-G14, G18, G21, G25	Averaged
- Hot leg temp. (K)	597.7 599.1	TF-HL1-03A TF-HL2-03A	Hot leg 1 Hot leg 2
- Cold leg temp. (K)	565.7 565.3 564.6 565.9	TF-CL1A-04A TF-CL1B-04A TF-CL2A-04A TF-CL2B-04A	Cold leg 1A Cold leg 1B Cold leg 2A Cold leg 2B
- RCS flow rate (kg/s)	2.2 ± 5% 2.2 ± 5% 2.3 ± 5% 2.2 ± 5%	QV-CL1A-01B QV-CL1B-01B QV-CL2A-01B QV-CL2B-01B	Cold leg 1A Cold leg 1B Cold leg 2A Cold leg 2B
- Core bypass flow rate (kg/s)	~0.0 ~0.0	Downcomer to upper head Downcomer to hot leg	Estimated value
- Pressurizer level (m)	3.4	LT-PZR-01	
Secondary system	(SG1/SG2)		
- Pressure (MPa)	7.85/7.85	PT-SGSD1-01/PT-SGSD2-01	Fig.4.1.12 of FDIR[1)] [12]
- Steam temp. (K)	566.9/566.3 568.6/569.3	TF-MS1-01/TF-MS2-01 TF-SGSD1-03/TF-SGSD2-03	Steam pipe line Steam dome
- FW temp. (K)	505.8/507.6 501.8/499.4	TF-MF1-03/TF-MF2-03 TF-MF1-04/TF-MF2-04	Economizer Downcomer
- FW flow rate (kg/s)	0.33/0.35 0.0/0.0	QV-MF1-01/QV-MF2-01 QV-MF1-02/QV-MF2-02	Economizer Downcomer
- Water level (m)	2.39/2.50	LT-SGSDDC1-01/ LT-SGSDDC2-01	Fig.4.1.18 of FDIR [12]
- Heat removal(MW)	0.693/0.774	-	Approximation
- Heat loss(kW)	28.5/28.5		Estimation
ECCS			
- SIT pressure (MPa)	4.23/4.23/4.22	PT-SIT1,2,3-02	
- SIT level (%)	314.2~314.8	TF-SIT1,2,3-03	
- RWT temp. (K)	92.0/91.3/90.4	LT-SIT1,2,3-01 (5.32/5.30/5.25)	Tag name/meter
- SIT temp. (K)	321.2	TF-RWT-01	Storage tank
Containment			
- Pressure (MPa)	0.1013	Atmospheric condition	Open

Note. 1) FDIR: ATLAS Facility Description and Instrumentation Report

2.3 Break Flow Estimated in the ATLAS DSP-01 Test

Detailed information on the major phenomena observed during the 100% DVI line break test can be found in the literature [5,11]. In this section, the test results of the break flow are discussed, which is important to the boundary conditions of the participants' calculations.

Regarding the break flow, a hybrid break flow was obtained as reference data. The load cell-based data showed more or less higher values than the RCS inventory-based data, especially in the beginning of the transient. The increasing gradient became smaller after the loop seal was cleared. Taking into account the measurement uncertainties of the two measuring methods, the load cell-based and the RCS inventory-based methods, it has been concluded that the RCS inventory-based measurement is more reliable than the load cell-based measurement in the early blow down period up to 452 seconds. But, this situation is reversed during the remaining test period. Therefore, hybrid break flow data was obtained by connecting the RCS inventory-based data with the load cell-based data at 452 seconds in order to provide reliable data for the break flow. The break flow rate and the accumulated break flow measured in the present SB-DVI-08 test are shown in Figs. 3 and 4.

2.4 Uncertainty Evaluation of the Measured Data

For the confidence of the measured data, uncertainty evaluations were performed for the major measurements, e.g. loop flowrate, collapsed water level, differential pressure, static pressure, and temperature. The uncertainty of the measured experimental data was analyzed in accordance with a 95% confidence level. According to the ASME's performance test code [13], the uncertainty interval of the present results was given by the root-mean-square of a bias contribution and a precision contribution. The bias and precision errors were evaluated from the data acquisition hardware specifications and the calibration results performed once every year, respectively. The estimated uncertainties are summarized in Table 4 and more detailed information can be found in reference 6.

3. EVALUATION OF PARTICIPANTS' CALCULATIONS

As shown in the Table 1, the MARS and RELAP5 codes were used for all the calculations. The RELAP5 code is a versatile and robust code based on a one-dimensional two-fluid model for two-phase flows. The COBRA-TF code, which is the base program for the MARS' 3-dimensional solver, employs a three-dimensional, two-fluid, three-field models. The MARS code is for a multi-dimensional and multi-purpose realistic thermal-hydraulic system analysis, in which the COBRA-TF is completely merged into the RELAP5 code.

In this section, the prediction results provided by ten

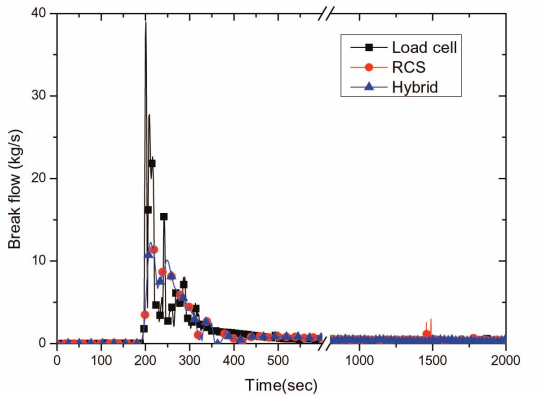

Fig. 3. Comparison of Estimated Break Flows

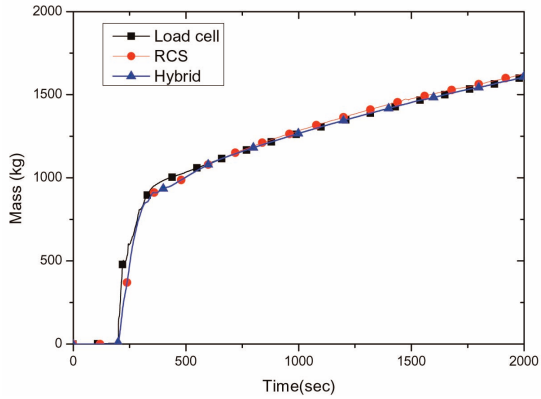

Fig. 4. Comparison of Estimated Accumulated Break Flows

Table 4. Summary of The Uncertainty Evaluation

Parameter	Error Level	Remark
Loop flow	± 15% of full span	Biflow flowmeter [14]
Collapsed water level	± 3.38% of full span	
Differential pressure	± 0.23 kPa	
Static pressure	± 0.039 MPa	
Temperature	± 2.4 K	

participants, i.e. KAERI, KEPRI, KINS, KOPEC, KNF, NETEC, SNU, KAIST, EN2T, and SDD were evaluated and compared with each other. The 100% DVI line break test of the ATLAS, SB-DVI-08 was analyzed by the participants by using the thermal-hydraulic system analysis codes, MARS-KS and RELAP5. The MARS-KS code was used by EN2T, KAERI, KAIST, KEPRI, KINS, SDD, and SNU and the RELAP5 code was used by KNF, KOPEC, and NETEC.

A steady-state input deck provided by KAERI was used by itself or modified according to the participants' needs. Some participants also revised the provided nodalization scheme (Fig.5) based on their previous experiences. The initial conditions acquired from their steady-state calculations were compared with the test results. In an overall sense, all the calculated steady-state results were in good agreement with the test data (within an acceptable discrepancy), except for a few minor disagreements by KAIST, KINS, SDD, and SNU. KEPRI performed a sensitivity study on the critical flow models with the options of the Henry-Fauske model, Ransom-Trapp model, and Moody model. Based on these steady-state results, transient analyses were performed. In most cases the predicted sequence of the major events was consistent with the test data, except for the loop seal clearing and the occurrence of peak cladding temperature (PCT). However, the opening characteristics of the main steam safety valve (MSSV) need to be improved by five participants (KAIST, KEPRI, KINS, SDD, and SNU). The feedwater injection and isolation logics should be checked again by KAIST and SDD, and several initial and boundary conditions of the core power, the safety injection actuation times, and loop seal clearing should be revised by SDD. The predictions of KOPEC, KNF, and KAERI (together with NETEC) showed relatively good agreement with the test data for the first opening time of the MSSVs, the core power with respect to time, and loop seal clearing phenomena. As the break flows were over-predicted in the EN2T and the NETEC calculations, the discharge coefficients at the break valve need to be adjusted for better prediction. As a sensitivity study, KNF modeled the pump suction legs in a more detailed manner to get a better prediction for the pump suction leg liquid level. KOPEC performed sensitivity calculations for the effects of the k-factor in the break line, the discharge coefficient of the break, and the RCP flow rate. KAIST modified the nodalization of the downcomer by using a double nodalization scheme with the top node linked with the bottom node. KAERI modeled the downcomer with 3-D nodalization using the MARS code.

A qualitative prediction performance of the submitted calculations will be discussed focusing on the important thermal-hydraulic parameters that have high relevance to safety in the next chapter. They include a comparison of the pressures, the fluid temperatures, the PCTs, the loop flow rates, the break flow rate, and the water levels. The following are some major findings from the participants and suggestions from the host organization.

1. (KAERI) The calculation showed that in an overall sense the MARS 3.1 code can predict the sequence of events and the major thermal hydraulic parameters of the primary pressure, the secondary pressure, and the injection flow rate with reasonable accuracy. The calculated PCT was 632 K at around 290 seconds due

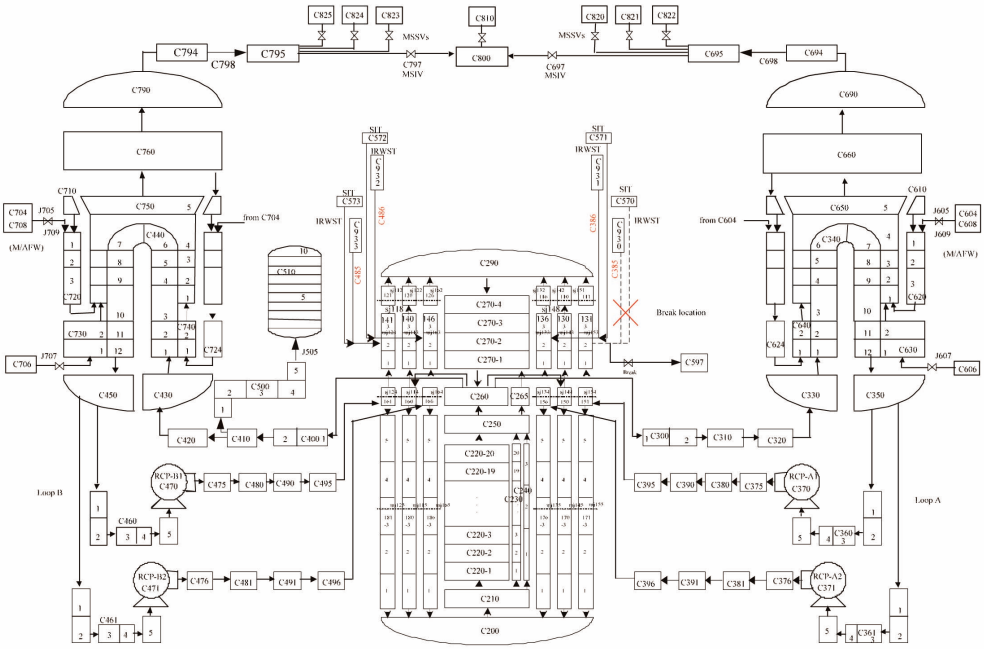

Fig. 5. MARS 1-D Nodalization for the SB-DVI-08 Test

to the reduction of the core water level. Except for the blowdown period, the calculated break flow rate properly agreed with the measured data.

2. (KEPRI) Their calculation overestimated the depressurization rate of the primary system and showed different trends in the prediction of the core heater surface temperature and the bypass flow rates through the hot leg to the downcomer.
3. (KINS) Their calculation result showed a reasonable prediction of the primary system behavior. However, the PCT and the active core level showed quite different trends compared to the measured data.
4. (KOPEC) The general trend of the calculation result was in good agreement with that of the test, but some disagreements, such as the large oscillation of safety injection flow rate and the high secondary system pressure were observed. Several sensitivity studies were carried out by KOPEC. The following is a summary of the sensitivity studies by KOPEC.
   A. The k-factor in the break line affected the friction in the break line. As the k-factor increased, the break flow rate decreased. The less break flow is predicted, the less PCT is. When the k-factor was greater than 1.0, no significant difference was observed.
   B. The discharge coefficient at the break also affected the break flow rate. Low discharge coefficient resulted in a decrease in the break flow rate, thus causing a low PCT. The discharge coefficient of 1.0 was used in the base case since it simulated the test data best.
   C. Initial pump speed affected the loop seal clearing time. As the initial pump speed at a steady-state condition decreased, the loop seal clearing was delayed and thus PCT was increased.
   D. The pump coast-down affected the loop seal clearing and the PCT. When the pumps were kept on, the loop seal clearing was delayed, but the PCT did not increase due to the forced circulation. The coast-down of the RCP was assumed in the base case simulation.
   E. The area change option at the break orifice affected the break flow rate. The smooth area change option resulted in more break flow and a higher PCT. The abrupt area change option fitted the test data better than the smooth area change option.
   F. The effect of the choking option at the break line was similar to the effect of the area change option. The choking option resulted in a lesser break flow rate and a lower PCT. Since the critical flow was observed at the break orifice, the choking option should be applied to the break line.
   G. The Trapp-Ransom critical flow model showed a delayed trend and a higher PCT than the Henry-Fauske model due to the smaller discharge flow during the blowdown. The Henry-Fauske model fitted the test data better than did the Trapp-Ransom model.
   H. Unlike the Henry-Fauske model, the effect of the area change option in the Trapp-Ransom model was small.
5. (KNF) The steady-state core bypass flows could not be obtained when six-channel downcomer modeling was used, but appropriate core bypass flows were obtained when a simpler, two-channel downcomer modeling was used. The code was able to predict (relatively well) the overall system behavior if the break flow was adjusted based on the system pressure. The code could not predict the behavior of the core collapsed liquid level before around 300 seconds and the significant over-prediction of the hot leg flows was thought to be the main reason for the over prediction. To improve the prediction for the hot leg flows, it might be necessary to investigate the input deck again focusing on the appropriateness of the flow resistances of each flow path. The code was not able to predict the behavior of the core collapsed liquid level after around 300 seconds mainly because the code had a tendency to predict the loop seal clearing with a large delay. As the core collapsed level was not predicted properly, the code over-predicted heater rod surface temperatures significantly. Even with a more detailed modeling of the pump suction legs, the complete and sudden loop seal clearing could not be predicted correctly. To see if a special model is necessary to take into account the higher mixing of safety injection water with steam in the downcomer, a calculation with arbitrarily increased interfacial heat transfer coefficients was conducted. For this calculation, the code was slightly modified to have 1,000 times larger interfacial heat transfer coefficients (HTCs) in the downcomer from the time of safety injection pump operation. However, such a modification was unable to improve the code predictions significantly. In other words, it was revealed that a special component to consider the high mixing of safety injection water with steam in the reactor vessel downcomer is not essential, at least not for the analysis of a DVI line break.
6. (NETEC) Overall, the prediction by the RELAP5 code was in reasonable agreement with the test data, even though a slight disagreement existed in the break flow prediction. Initial analysis results, especially, showed that the break flow predicted by the RELAP code was considerably different from the test data. Although they adjusted the break flow by improving the discharge coefficient adequately, the calculation results still presented a disagreement for the break flow.
7. (SNU) The calculation by the MARS code predicted the test data with reasonable accuracy. However, the calculated PCT showed different trends compared with the test data. The deviation was due to the timing and the period of the core uncovery. The core water level was affected by the downcomer water level and the differential pressure between the core and the

downcomer. Because the balance of the phenomena in the core and the downcomer was not predicted properly with the MARS code, the water level and the PCT showed different trends.

8. (KAIST) They identified the following major problems with the MARS prediction: Either no or too much delayed loop seal clearing in the vertical intermediate legs; different PCT time/elevation locations and its duration time; under-predicted core/downcomer collapsed water level; over-predicted cold leg flow rate; over-prediction of steam generator heat removal rate; over-prediction of steam generator dome pressure. Because the PCT (591 K) and its duration time (about 50 seconds) adopting double nodalization in the downcomer were closer to the measured data than to the MARS analysis results [5] (e.g. PCT of 743 K, more than 150 seconds of PCT duration time), they recommended the double nodalization scheme for the nodalization of the downcomer.
9. (EN2T) They applied a CCFL option to the upper guide plate above the active core region and succeeded in predicting the PCT with reasonable accuracy. Their MARS-KS code calculation showed some discrepancies in predicting the core level, the loop seal clearing, and, consequently, there was a large difference in the PCT behavior. They concluded that further analyses on the condensation heat transfer model and the loop seal clearing phenomena are required in order to investigate the root cause of the discrepancies. The level tracking model was also addressed for improvement in order to calculate the mixture level.
10. (SDD) As several initial and boundary conditions were not in agreement with the test data, significant disagreements in the transient results were obtained. The initial and the boundary conditions should be revised and the transient results should again be discussed based on them.

Computational CPU times up to 1000 seconds were compared with each other (refer to Figure A-87 in the reference 6). Among the calculations, the KEPRI's, KINS's, and SDD's results showed a much longer CPU time than the others. This difference seemed to be attributable to modeling differences, especially in the break system as well as in the ECC injection system. Usually, experienced users have a capability to optimize their computational time by applying efficient modeling to specific components. The time step up to a specified transient time varied from around 1E-4 to 0.05 seconds depending on calculations (refer to Figures A-88 through A-90 in the reference 6).

4. COMPARISON OF CODE CALCULATIONS

4.1 Comparison of Initial and Boundary Conditions

The initial and the boundary conditions used by all the participants are listed in Table 5. Key parameters among the requested parameters were selected and compared with the data in order to check whether the calculations were performed in a manner consistent with that of the actual test conditions.

In general, most participants appropriately simulated the initial conditions of the test. Some participants, however, did not manage to achieve the same initial condition of the data for a certain parameter. For instance, KAIST did not properly simulate the feedwater flow rate. KINS calculated extremely higher containment pressure than the data. SDD and SNU could not initialize the initial conditions of the SIT appropriately.

4.2 Sequence of Events

Table 6 shows the sequence of events calculated by the participants and comparisons with the data. Most participants assumed that the break was initiated at 0.0 second but a few participants used a similar break initiation time around 199 seconds into the test. In order to summarize the sequence of events in calculations and to compare them with the data, the submitted calculation times and test times were adjusted for the break time to be 0.0 second. The MSSV opening characteristics were modeled by only four participants out of the ten participants. The other five participants need to improve their calculations by considering the actual MSSV characteristics. With regard to the first opening time of the MSSVs, there were some discrepancies with the data. KOPEC's predictions were outstanding in terms of their accuracy.

The LPP trip times, in general, were accurately predicted by all calculations. The RCP trip time has no special importance for the current transient because the RCP was operated in a free running condition from the beginning of the present test. The initial condition of the test was achieved in a natural circulation mode. Therefore, the RCP trip time of 25 seconds in the test did not effect any change in the RCS flow rate. All participants are advised to check whether their calculations were based on the actual test condition.

The main steam isolation valve (MSIV) closure times could not be obtained from the submitted calculations due to the limited parameters requested. In the SB-DVI-08 test, the MSIV was closed with a delay of 0.1 seconds after the LPP. All participants are advised to check the actuation of the MSIV in their calculations. The main feedwater was also isolated with a delay of seven seconds after the LPP in the test. Most calculations correctly simulated the isolation of the main feedwater in connection with the LPP signal, but the main feedwater isolation was not actuated in SDD's calculation. They need to check the trip variables in their calculations. KAIST did not simulate the feedwater injection during their entire calculation period.

The core power with respect to time was provided to all participants as a boundary condition. However, the calculated core powers were not consistent with the data

Table 5. Comparison of Initial Conditions

	Experiment	KAERI	KEPRI	KINS	KOPEC	KNF	NETEC	SNU	KAIST	EN2T	SDD
Primary system											
Core power, MW	1.647	1.553	1.566	1.545	NA	1.555	1.565	1.552	1.540	1.566	1.539
Pressure, MPa	15.49	15.60	15.51	15.51	15.51	15.47	15.51	15.52	15.51	15.54	15.51
Core inlet temp., K	563.2	563.2	563.8	563.8	563.3	564.7	563.8	563.8	563.8	563.8	563.8
Core exit temp., K	598.9	598.2	597.3	596.9	598.8	599.2	596.9	596.9	597.3	596.8	597.3
Bypass UH-DC, kg/s	~0.0	0.029	0.008	-0.015	0.0	0.039	0.025	-0.024	0	-0.02	-0.012
Bypass HL-DC, kg/s	~0.0	0.018	0	0.024	-0.002	0.11	0	0.021	-0.047	0.056	0.012
CL flow rate, kg/s	2.2	1.93	2.01	0	1.88	1.96	2.01	1.99	2.01	2.02	2.01
PZR level, m	3.4	3.54	4.11	4.04	3.57	3.40	4.12	4.04	3.52	4.01	4.04
Secondary system											
Pressure, MPa	7.85	7.88	7.83	7.83	7.81	7.83	7.82	7.83	7.83	7.83	7.83
Steam temp., K	569.0	566.2	566.6	566.6	566.5	566.7	566.6	566.6	566.6	566.6	566.6
FW flow (ECO), kg/s	0.34	0.455	0.400	0.400	0.445	0.323	0.400	0.400	0	0.400	0.400
FW flow (DC), kg/s	~0.0	0	0.044	0	0	0	0.044	0.044	0	0.044	0.044
Heat removal, kW	733.5	809.7	781.7	780.1	783.5	758.5	804.1	773.4	780.7	780.0	780.1
ECC											
SIT pressure, MPa	4.23	4.21	4.03	4.23	4.23	4.23	4.23	0	4.23	4.23	4.20
SIT Temp., K	314.6	323.5	322.0	324.2	320.9	324.1	324.3	323.9	323.2	325.0	563.7
Containment											
Pressure, MPa	0.10	0.10	0.10	15.56	0.10	0.10	0.10	0.10	0.10	0.0	0.10

Table 6. Summary of Calculated Sequence of Events

		Exp.(Shifted time, sec)	KAERI	KEPRI	KINS	KOPEC	KNF	NETEC	SNU	KAIST	EN2T	SDD
Break		0.0	0.0	0.0	0.0	0.0	0.0	0.0	0.0	0.0	0.0	0.0
1st MSSV open		16.0	25.0	NO[1)]	NO	16.6	9.02	25.0	NO	NO	NO	NO
LPP trip		20.0	22.04	19.04	18.35	23.28	21.0	22.0	22.0	21.35	20.7	27.35
RCP trip		20.0	22.04	19.39	18.35	23.28	21.35	22.0	22.0	21.35	21.05	27.35
MSIV closure		20.0	21.76	19.14	NA	23.0	NA	NA	NA	NA	20.77	NA
MFW isolation		27.0	28.75	26.11	25.0	30.0	28.07	28.0	28.0	NA	27.77	NO
Core decay		24.0	24.0	19.39	20.0	NA	20.02	22.0	26.0	23.05	24.7	NA
Max. PCT		91.0	232	245.5	280	255	350	NO	277	NO	290	NO
SIP activation		47.0	49.97	47.32	50.0	51.21	50.0	50.0	48.0	51.0	50.0	58.0
SIT activation		232.0	228.3	179.8	230.0	237.3	240.0	233.0	233.0	248.0	232.0	58.0
Loop seal	CL1A	88.0	79.0	NO	1020	NO	101.0	86.0	NO	NO	105.0	NO
	CL1B	88.0	79.0	77.0	NO	211.0	101.0	86.0	89.1	92.0	105.0	NO
	CL2A	109.0	79.0	47.0	95.0	211.0	91.0	85.0	90.1	90.0	104.0	NO
	CL2B	109.0	79.0	47.0	95.0	231.0	101.0	85.0	91.1	90.0	104.0	NO
Stop		2000	2000	2000	1250	2000	1000	2000	2000	2000	2000	1200

Note 1) Did Not Occur

in most calculations. Only KAERI's predictions were outstanding in terms of their accuracy. KOPEC did not submit the core power calculation data and there was serious error in modeling the core power in SDD's calculation.

The actuation times of the SIP and the SITs depend on the depressurization rate of the primary system, so the actuation times showed a difference from the calculation results.

Loop seal clearing is an important phenomenon of the present test since its timing significantly influences the core mixture level and the PCT. In the test, the loop seals of all the intermediate legs were cleared with some time differences. KOPEC's and NETEC's predictions showed a relatively good agreement with the test data even though they showed a slight time deviation in the occurrence time. In SDD's calculation, not one intermediate leg was cleared.

4.3 Transient Results

The transient calculation results were qualitatively compared with the measured data. All the compared figures are included in Appendix-A of the comparison report [6]. In this section, a qualitative prediction performance of the submitted calculations is described, focusing on the important thermal-hydraulic parameters that have high relevance to the safety.

In the SB-DVI-08 test, the primary system pressure rapidly dropped to about 8.2 MPa from its initial pressure of 15.5 MPa at the break. The decreasing rate of the primary system pressure became small at around 50 seconds after the break. No obvious plateau region of the primary system pressure was observed, implying that the effects of the loop seal on the primary system pressure were not so significant in the present test. Most calculations properly predicted the initial pressure drop behavior after the break. KEPRI's calculation, however, overestimated the depressurization rate of the primary system pressure and SDD's prediction presented the overestimated depressurization rate and the fluctuations of the primary system pressure.

In the present SB-DVI-08 test, due to the main feedwater isolation subsequent to the reactor trip, the secondary pressure started to increase up to the MSSV set-point, 8.1 MPa. Three MSSVs were installed parallel to each steam line. In the test, OV-MSSV1-03 at the SG-1 line and OV-MSSV2-03 at the SG-2 line were opened, once at 215 seconds and twice at 215 and 242 seconds, respectively. The other two MSSV banks were not actuated. The increase in the secondary pressure was depressed only by the opening of one bank of the MSSVs. In general, the prediction performances of the secondary system pressure by the participant's calculations were unsatisfactory (contrary to the primary system pressure prediction). Only four participants, KAERI, KNF, KOPEC, and NETEC predicted the opening of the MSSV. The other six participants need to improve their calculations by considering the actual MSSV characteristics. With regard to the first opening time of the MSSVs, KOPEC's predictions were outstanding. KAERI's and NETEC's calculations predicted the opening of the MSSV once. On the other hand, KNF's and KOPEC's calculations predicted the opening of the MSSV five times and six times, respectively. Since the MSSV was not pertinently simulated in most calculations, the secondary system pressure maintained a relatively higher value compared to the test data.

4.3.1 Pressure Comparison

In the SB-DVI-08 test, the containment pressure increased up to 0.24 MPa from its initial pressure of 0.1 MPa at the break. As for the prediction performance of the containment pressure, the calculations performed by SNU, NETEC, KAIST, KNF, and KOPEC showed relatively excellent simulations. The other calculations did not show any variations of the containment pressure during the whole test period. They seemed to use a constant containment back-pressure in their calculations. KINS calculated the pressure of the containment as extremely high. They set the initial pressure of the containment at 15.56 MPa, similar to the primary system pressure.

4.3.2 Fluid Temperature Comparison

The core inlet and exit temperatures were requested as important fluid temperatures. Until the time of 100 seconds from the break, when the second depressurization started, most calculations showed reasonable predictions of the core inlet and exit temperatures, as shown in Figs. 6 and 7. After this initial period, the predictions showed a wide range of variation, and the deviation from the test data increased with time. On the whole, the largest discrepancy was observed in SDD's calculation, which underestimated the fluid temperatures initially and showed a highly fluctuating behavior, especially after about 300 seconds. In general, the core temperatures were underestimated by EN2T and KEPRI, and overestimated by the other participants. As for the prediction of the core fluid temperatures, KINS's calculations showed outstanding accuracy.

Each calculated hot leg fluid temperature showed the same trend as the core outlet temperature. In general, the hot leg fluid temperatures were underestimated by EN2T and KEPRI, and overestimated by the other participants. The measured cold leg temperatures showed asymmetrically different behavior depending on the loop. A sudden increase in the water temperature indicated that the water in the cold legs 1B, 2A, and 2B was emptied by steam flow. This cold leg fluid temperature behavior was not simulated in any calculation. The best prediction of the hot leg and the cold leg temperatures was obtained in KINS's calculation.

The steam dome temperatures were predicted in the range of a 10 K deviation in most calculations. During the

initial period up to 200 seconds, an underestimation of the steam dome temperatures was prevailing and thereafter they were overestimated in most calculations. The SIT fluid temperatures were relatively well simulated for most calculations within +/- 3.0 K, except for SDD's calculation. The initial fluid temperatures of the SIT were assumed to be quite high in SDD's prediction and they presented abnormal behavior with high fluctuations. As for the fluid temperature of SIP-2, it experienced a small fluctuation at the initial injection period in the SB-DVI-08 test. SNU's calculation showed the best prediction performance for the SIP fluid temperature. The other calculations except for SDD's calculation presented constant fluid temperatures with a reasonable accuracy.

4.3.3 PCT Comparison

The core heater surface temperatures (represented by the wall temperature in the active core regions) were compared with the test data and the calculations. The active core region was instrumented at twelve elevations from the core inlet to the core outlet to measure the core heater temperatures. In this section, the core wall temperatures were compared with respect to three representative regions along the core, e.g. region 2, region 7, and region 12.

In the lower region (region 2), most calculations showed quite good predictions, but SDD's calculations presented a constant temperature of about 600 K during the whole test period. They showed the same temperature behavior of the core heater surface in all the core regions. They need to check their input model precisely for the heat structure and the heat transfer in the core regions. KEPRI's calculation consistently underestimated the wall temperature after a time of 100 seconds. In the later period (from the time of 800 seconds), most calculations, except for KEPRI's prediction, slightly overestimated the wall temperature.

In the middle region (region 7), five calculations performed by EN2T, KEPRI, KINS, KNF, and KOPEC showed one or multiple PCTs around 90 ~ 600 seconds and the other calculations did not present the excursion of the core wall temperatures. KOPEC's calculation showed multiple peaks of the core wall temperatures. In KEPRI's calculation, the heat-up of the core was maintained for a long period of about 400 seconds. In terms of the magnitude and timing of the PCT, EN2T's calculation showed an outstanding prediction performance in the middle region of the core.

In the higher region (region 12), most calculations, except for NETEC's prediction, showed PCTs around 110 ~ 700 seconds, as shown in Fig. 8. In this region, most of the PCTs showed quite long quenching times. The best prediction of the core wall temperatures for this region was obtained in NETEC's calculation.

4.3.4 Loop Flow and Break Flow Comparison

In the SB-DVI-08 test, the bypass flow rates were simulated to preserve the bypass behavior of the APR1400 as realistically as possible. The bypass flow rates were controlled to provide the scaled values through the bypass

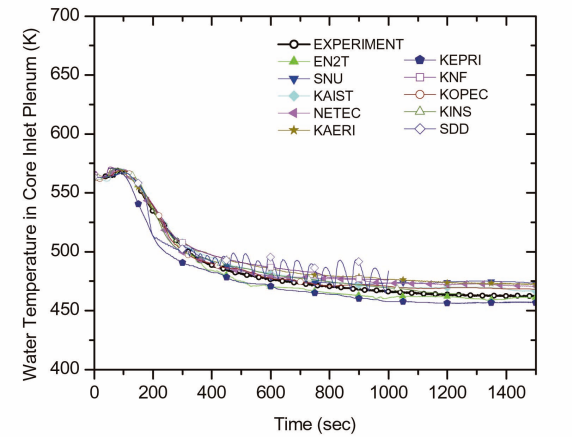

Fig. 6. Comparison of Water Temperature in Core Inlet Plenum

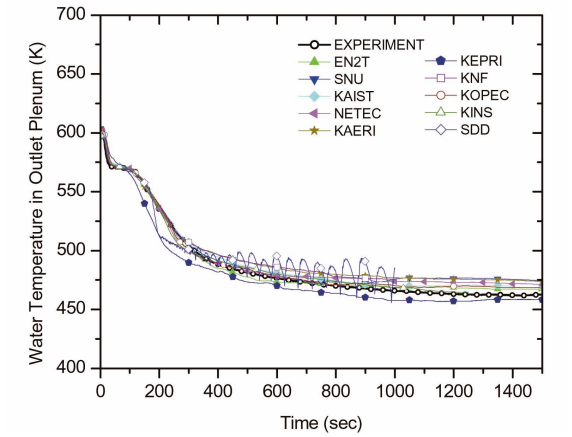

Fig. 7. Comparison of Water Temperature in Core Outlet Plenum

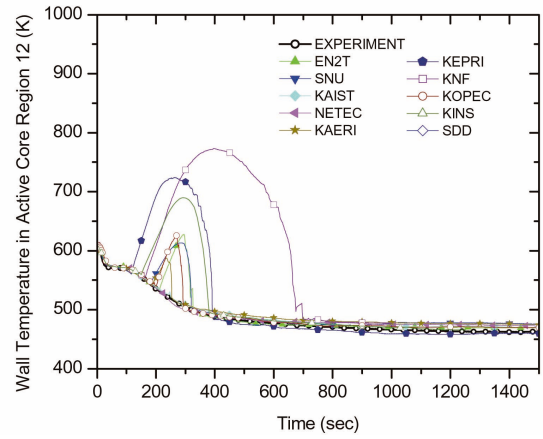

Fig. 8. Comparison of wall Temperature in Active Core Region (Region 12)

flow lines based on the performance tests for the four bypass valves connected to the downcomer. The two bypass valves of FCV-RV-37 and FCV-RV-38 between the downcomer and the upper head were opened by 74% and 65%, respectively, to provide the required flow rate of 0.25 kg/s each and the two bypass valves of FCV-RV-95 and FCV-RV-96 between the downcomer and the hot legs were opened by 81% and 97%, respectively, to provide the required flow rate of 0.71 kg/s each. Therefore, the flow rates through the upper head to the downcomer and the hot leg to the downcomer bypass lines are estimated to be 0.5 and 1.42 kg/s, respectively. All the predictions underestimated the bypass flow rates through the upper head to the downcomer bypass lines. The calculations performed by EN2T, KNF, KOPEC, NETEC, SDD, and SNU presented the opposite flow direction to that in the test data. KAIST's calculation predicted a zero bypass flow rate and KINS's calculation showed fluctuations in the flow direction. Only KAERI's calculation predicted the same flow direction as that in the test data. Most predictions underestimated the bypass flow rates through the hot leg to the downcomer bypass lines, except KEPRI's prediction. Only KAIST's calculation reproduced the same flow direction as that in the test data. KEPRI's calculation, in particular, presented the highly oscillated bypass flow rate through the hot leg to the downcomer.

In the present SB-DVI-08 test, the flow rates in the two hot legs and four cold legs were measured by using BiFlow flow meters. All the predictions estimated the test data correctly in an overall sense. However, most predictions showed fluctuations during the latter period for hot legs 1 and 2, and the predictions were higher than the test data during the initial period for cold legs 2A and 2B.

The flow rates through the main feedwater lines were measured by using Coriolis flow meters. All the calculations predicted the test data correctly in an overall sense. KAIST and SDD, however, did not properly simulate the feedwater flow rate. In SDD's calculation, the feedwater flow rate maintained the initial value without the actuation of the main feedwater isolation valve. The feedwater flow was not supplied during the whole test period in KAIST's calculation.

The flow rates from three SITs and one SIP were also measured by using the Coriolis flow meters. Most calculations overestimated the flow rates from the three SITs. In particular, SDD's calculation presented a highly oscillating flow rate and an earlier injection of the SIT compared with the test data. In NETEC's calculation, only the SIT-1 was actuated. All the calculations slightly overestimated the flow rate from the one SIP and SDD's calculation showed remarkable fluctuations of the flow rate.

In the SB-DVI-08 test, the total break flow rate was calculated by using the measured data of QV-CS-03, LC-CS-01 and LC-CS-02. Most calculations, except for SDD's prediction, predicted the test data correctly in an overall sense, as shown in Fig. 9. In the present test, the accumulated water mass for break flow was measured by two load cells. SDD's calculation presented a zero accumulated mass of break flow for the whole test period. KAERI's and KEPRI's calculations relatively overestimated and underestimated the accumulated mass of break flow, respectively.

4.3.5 Water Level Comparison

In the SB-DVI-08 test, the collapsed water level of the downcomer experienced a sudden drop with the opening of the break valve. This water level was maintained until just before the loop seal clearing. It significantly decreased afterwards until the SIT injection started. With the actuation of the SIT injection, the collapsed water level slowly increased again. This general trend could be observed in all the calculations, as shown in Fig. 10. However, the occurrence time of the loop seal clearing and the decreasing

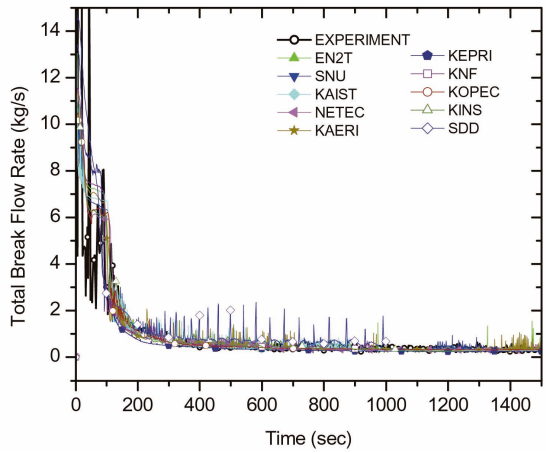

Fig. 9. Comparison of Total Break Flow Rate

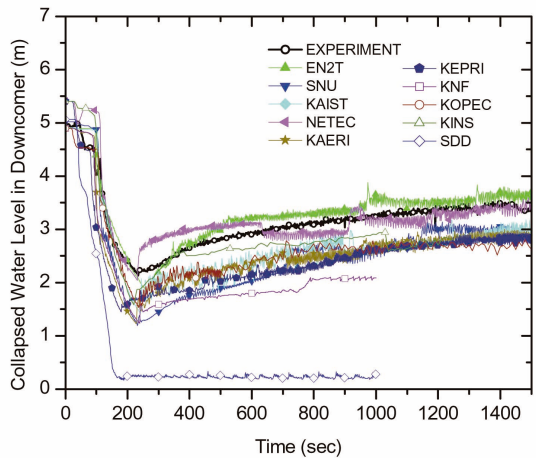

Fig. 10. Comparison of Collapsed Water Level in Downcomer

rate of the water levels were different depending on the participant. Except for EN2T's and NETEC's calculations, the collapsed water levels of the downcomer were underestimated during the later period after the SIT injection.

With regard to the core water level, temporary core level depression was observed in the present test when the loop seal clearing occurred. After that, the core water level was maintained at a constant level during the remaining test period. In general, most calculations showed very fluctuating results and no calculations predicted the data correctly with a satisfactory accuracy, as shown in Fig. 11. Among the calculations, EN2T's calculation predicted the initial core level depression with an outstanding accuracy and KAERI's calculation predicted the core water level during the latter period (after 300 seconds) with a reasonable accuracy.

The water in the vertical intermediate leg-1A and -1B was cleared and the first loop seal clearing occurred at 88 seconds after the break in the present test; then, the other two loop seals of leg-2A and -2B were cleared at 109 seconds. KOPEC's and NETEC's predictions showed a relatively good agreement with the test data even though they showed a slight deviation in the occurrence time. In SDD's calculation, none of the intermediate legs was cleared. In the predictions of EN2T, KAIST, KEPRI, KINS, and KNF, loop seals were cleared only in the three intermediate legs. The collapsed water levels in the intermediate legs were closely related to the loop seal clearing phenomena and also the collapsed water level behavior of the core and the downcomer.

The collapsed water levels in the U-tube region were relatively well predicted in most calculations except for KINS's calculation. In KINS's prediction, the collapsed water levels in the U-tube did not vary during the whole test period. In general, the water levels of the downward section decreased more rapidly than those of the upward section both in the test and in the calculations.

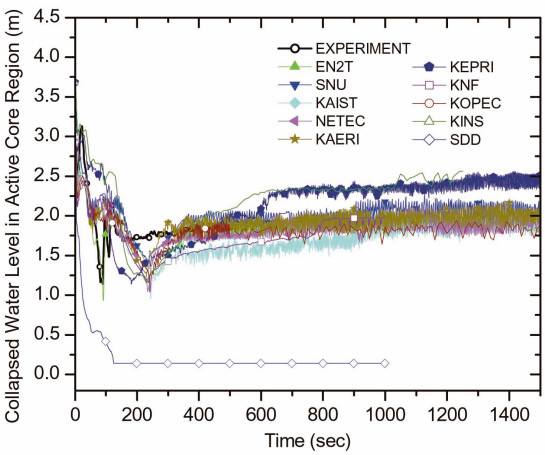

Fig. 11. Comparison of Collapsed Water Level in Active Core Region

5. ACCURACY QUANTIFICATION

5.1 FFTBM Methodology

Qualitative comparison of the submitted calculation results against the measured data was described in the previous section of this paper. And in order to determine a clearer quantification of the prediction performance, a methodology proposed by F. D'Auria at the University of Pisa (DCMN), FFTBM (Fast Fourier Transform Based Method) [15~18] was applied to the present DSP-01 exercise. FFTBM is an integral method using the Fast Fourier Transform (FFT) in order to represent the code discrepancies in the frequency domain. This method has been successfully applied to past International Standard Problems (ISPs) or Standard Problem Exercises (SPEs) organized by CSNI or IAEA in order to quantify the prediction accuracy of the codes used in the program [19]. A good review can be found in the literature [20].

5.2 Application to the DSP-01 Exercise

A combination of the average amplitude (AA) and weighted frequency (WF) are used as a Figure Of Merit (FOM) to characterize the accuracy of a given calculation. In order to apply the FFTBM to the present DSP-01 exercise, a few parameters, which affect AA and WF, should be decided on: the number of variables to characterize the scenario (N_{var}), the analysis time frame (T_d), the number of points (N), the cut-off frequency (f_{cut}), and the weighting factors for overall accuracy quantification (w_f)

5.2.1 Selection of Parameters and Weighting Factors

A total of 86 thermal-hydraulic parameters were requested in the DSP-01. Usually, the full FFTBM method requires 20-25 parameters selected to represent the relevant thermal-hydraulic aspects. By personal communication with D'Auria's group, 22 parameters have been selected to characterize all the relevant phenomena that were measured during the test, as shown in Table 7. Similar parameters that would affect the analysis results and the parameters that have great measurement uncertainties have been avoided in this selection process.

The weighting factors were used to consider the different importance from the viewpoint of the safety analysis and to determine the overall accuracy of the calculation, i.e., the total average amplitude (AA_{tot}). In the present analysis, the weighting factors used in Table 1 of the reference 20 were adopted. The weighting factors used in the present analysis are listed in Table 7.

5.2.2 Cut-Off Frequency Selection

The cut-off frequency means the highest frequency to which the average amplitude (AA) and weighted frequency (WF) are calculated in the FFTBM. The AA and WF

depend on the cut-off frequency. High frequency errors are more acceptable than errors caused by low frequency components. Thus, a sensitivity study of the impact of the cut-off frequency on AA and WF was carried out. It was found that a frequency higher than 1.0 Hz had no significant impact on the AA and WF. Consequently, 1.0 Hz was taken as the cut-off frequency for all the selected parameters in the present analysis.

5.2.3 Selection of Time Interval and Amount of Data

The amount of data (N) should be a power with a base equal to 2 to perform FFT calculations. The selection of the amount of data also depends on the time interval of the calculation. A minimum calculation time of 1000 seconds was required in the present DSP-01 exercise because the most important phenomena took place within 1000 seconds. The amount of data needs to be large enough to include a high frequency effect on the final AA_{tot} but does not need to be so large as to include frequencies higher than the cut-off frequency. So, the amount of data was determined by taking the time of the interval into account.

As for the time of interval for the present analysis, the transient behavior of the DVI line break scenario should be identified from a viewpoint of phenomenology. According to the PIRT (Phenomena Identification Ranking Table) performed for the DVI line break, the transient behavior can be categorized into four phases: pre-trip phase, post-trip phase, refill phase, and long term cooling phase [21].

Based on the PIRT results and observed phenomena in the SB-DVI-08 test, three time intervals were selected to perform the FFTBM, as shown in Table 8. The time of 24 seconds was selected as the first time of interval relevant to the pre-trip phase. This time frame focuses on the prediction accuracy comparison during the initial blowdown period at a constant power condition. Despite a very short time of 24 seconds, we sampled 512 bits of data for the

Table 7. Weighting Factor Components for the Analyzed Parameters

Parameters		Instrument Name	Weighting factor			
			w_{exp}	w_{saf}	w_{norm}	w_f
Core power	D1[1)]	Σ HP-CO-0i-P	0.8	0.8	0.5	0.32
Pressurizer pressure	D5	PT-PZR-01	1.0	1.0	1.0	1.00
SG1 steam dome pressure	D6	PT-SGSD1-01	1.0	0.6	1.1	0.66
SIT-01 pressure	D8	PT-SIT1-02	1.0	0.6	1.1	0.66
Core inlet temperature	D16	TF-LP-2G18	0.8	0.8	2.4	1.536
Core exit temperature	D17	Averaged	0.8	0.8	2.4	1.536
Clad temp. at region 2	D43	TH-CO-02G11a1	0.9	1.0	1.2	1.08
Clad temp. at region 7	D48	TH-CO-07G11a1	0.9	1.0	1.2	1.08
Clad temp. at region 12	D53	TH-CO-12G11a1	0.9	1.0	1.2	1.08
Hot leg 1 flow rate	D56	QV-HL1-01A+B	0.5	0.8	0.5	0.20
Hot leg 2 flow rate	D57	QV-HL2-01A+B	0.5	0.8	0.5	0.20
Active SIT-01 flow rate	D66	QV-SIT1-01	0.5	0.8	0.5	0.20
Active SIP-02 flow rate	D69	QV-HPSI1-03	0.5	0.8	0.5	0.20
Total break flow rate	D70	Calculated	0.5	0.8	0.5	0.20
Accumulated break mass	D71	Integral of D70	0.8	0.9	0.9	0.648
Downcomer level	D72	LT-RPV-04A	0.8	0.9	0.6	0.432
Active core region level	D73	LT-RPV-01	0.8	0.9	0.6	0.432
Pressurizer level	D74	LT-PZR-01	0.8	0.9	0.6	0.432
Collapsed water level IL1A	D75	LT-IL1A-03	0.8	0.9	0.6	0.432
Collapsed water level IL1B	D76	LT-IL1B-03	0.8	0.9	0.6	0.432
Collapsed water level IL2A	D77	LT-IL2A-03	0.8	0.9	0.6	0.432
Collapsed water level IL1B	D78	LT-IL2B-03	0.8	0.9	0.6	0.432

Note 1) Data Group Number Defined in Reference 6

FFT calculation according to a suggestion in the literature [20], resulting in a maximum frequency up to 10.66 Hz. The sampling process was done by a linear interpolation of the calculation data and of the test data.

The second interval was selected as the time up to which the SITs were actuated. In this time frame, all the important thermal-hydraulic phenomena are expected to occur, including the interaction of the break flow with the ECC flow by SIP. Also, the loop seal clearing was expected to happen. A total of 1024 bits of data in the second interval were sampled by a linear interpolation of the calculation data and the test.

The third interval was selected to cover the entire phenomena relevant to the DVI line break scenario. The most meaningful phenomena took place in less than 1000 seconds even though the test was carried out up to 4054 seconds. So, a period of 1000 seconds was selected as the third time frame for the present FFTBM assessment. This period corresponds to the refill and long term cooling phase defined in the PIRT activity. In this third interval, a total of 4096 bits of data were sampled by the same interpolation method that was used in the previous interval.

5.3 Accuracy Evaluation Results for DSP-01 Exercise

For each participant, three cases with different time frames were calculated. In the first time frame between 0.0 second to 24 seconds, three parameters relevant to the SIP and SIT were excluded in the FFTBM calculation because the SIP and SIT were not available during this period. In the second time frame between 0.0 second to 230 seconds, two parameters relevant to the SIT were excluded because the SIT was not activated in this interval. In the entire time frame calculation, the 22 selected parameters were used to calculate the final AA_{tot}. A summary of the FFTBM evaluation results can be seen in Table 9. The participants who submitted their calculations are designated as A1 through A5 and B1 through B5 in the divided group. In this section, all the participants are described anonymously.

In the literature, the accuracy of a given calculation is characterized by the following criteria [19]:

$AA_{tot} = 0.3$: very good prediction
$0.3 < AA_{tot} < 0.5$: good prediction
$0.5 < AA_{tot} < 0.7$: poor prediction
$AA_{tot} > 0.7$: very poor prediction

In the first time frame, most calculations resulted in very good prediction of the data except for B5's calculations. The obtained AA_{tot} were significantly lower than the acceptable criterion ranging between 0.1 and 0.16. Overall, the best prediction was obtained in the calculation by A1 (AA_{tot}=0.129). A4's and B3's calculations, respectively, were excluded in the overall assessment because core power and hot leg flow rates were not submitted. If we looked at the detailed results for each parameter, a major discrepancy could be seen to originate from the incorrect prediction of the hot leg flow rates, especially in hot leg 2. The total break flow rate was also a major source of disagreement. The collapsed water levels in the downcomer were excellently reproduced in most calculations. But, most AA_{tot} values for the active core region showed relatively higher values, by at least an order of magnitude.

In the second time frame, the effect of the SIP injection flow was added to the first time frame. But, the impact of the SIT on the prediction accuracy was still excluded. The most significant thermal-hydraulic phenomena occurred in this time frame. Like the first time frame results, most calculations showed good predictions in this time period. Just like in the first time frame, most disagreements originated from the hot leg flow rates and the break flow. Even though the total break flow rates were predicted with poor accuracy in most calculations, the accumulated break flow rates were fairly well predicted. Most participants seemed to do their best to obtain an accumulated break flow rate consistent with the test data. At this moment, it is very difficult to reach the conclusion that they failed to reproduce the consistent break flow rate because the test data itself also included some uncertainty in measuring the break flow rate. In this time frame, disagreements about the collapsed water levels of the vertical intermediate legs become remarkable. In the SB-DVI-08 test, four loop seals were rapidly cleared almost simultaneously, but most

Table 8. Selected Time of Interval for the Present FFTBM Analysis

Time of interval	Phase relevant to PIRT	Phenomena observed	Number of data	Max. frequency $f_{max}=0.5f_s$(Hz)
0~24 seconds	Pre-trip	Before the core power decay Core power decay at 24 seconds in the test	512	10.66
0~230 seconds	Post-trip	Before the SIT injection SIP injection at 47 seconds in the test SIT injection at 232 seconds in the test 1st loop seal clearing at 82 seconds in the test	1024	2.23
0~1000 second s	Refill and long term cooling	All the interesting phenomena are included in this time frame	2048	1.02

calculations showed a smooth clearing. This disagreement was the major cause for higher AA_{tot} values. As for the prediction of PCT, the PCT at region 2 was reasonably predicted in most calculations. But, the PCTs at regions 7 and 12 were poorly predicted (refer to Fig. 8 for region 12). Unlike the actual test results, many calculations predicted an increase in the PCT up to about 800 K.

The third time frame includes the most meaningful transient phenomena in the present test. Compared with the previous second time frame, the influence of the SIT injection on the transient behavior was taken into account in this time frame. AA_{tot} values for the active SIT-01 flow rate show values much higher than 1.0 except for B2's calculation. B2's prediction of the SIT-01 flow rate (AA_{tot}=0.313) was outstanding among the other calculations. In the present test, the measured SIT flow rate showed an oscillating behavior. The ECC water by the SIT was very low because the pressure difference between the SIT and the upper downcomer, which is a driving force to inject the ECC water into the core, was not so high. Thus, this oscillation is thought to be attributable to condensation of the vapor in the downcomer region, which is due to injected cold water. Most calculations modeled the SIT flow rate with the same empirical relationship between the downcomer pressure and the SIT flow rate to that used in the test. However, this modeling seems not to take account of the condensation-induced oscillation phenomena in the downcomer. In conclusion, the prediction capability of the SIT flow rates was very poor in most calculations.

The FFTBM results applied to the DSP-01 are summarized in Table 9 and Fig. 12. Overall, most calculations showed very good prediction results except for one calculation. This FFTBM is based on several assumptions: selection of variables, selection of time frame of interest, weighting factors, and cut-off frequency. These assumptions are rather more subjective than objective so that the ranking among the calculations may be changed if different assumptions are used. Therefore, the rankings in Table 9 and Fig. 12 do not mean a definite superiority of one calculation over the other calculations. However, when the present assumptions are used, the best and the worst calculations were provided by participants B3 and B5, respectively. By comparing with the qualitative comparison

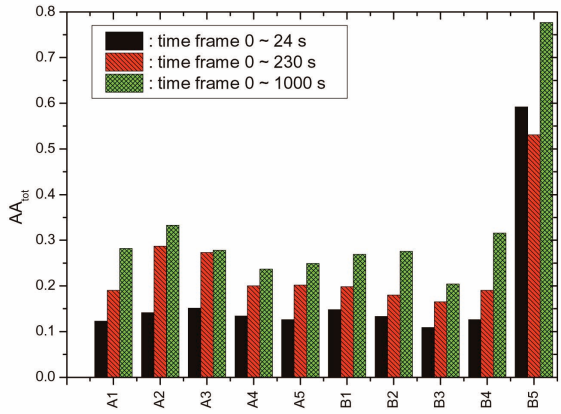

Fig. 12. Comparison of the Prediction Accuracy of The Participants Based on FFTBM

Table 9. Summary of the Results of FFTBM to DSP-01 Calculation

Group	Participant/Code		Time of interval					
			0 ~ 24 s		0~ 230 s		0 ~ 1000 s	
			N=512		N=1024		N=2048	
			AA_{tot}	WF_{tot}	AA_{tot}	WF_{tot}	AA_{tot}	WF_{tot}
A	A1	MARS-KS	0.123	0.149	0.190	0.108	0.282	0.109
	A2	MARS-KS	0.141	0.128	0.287	0.108	0.333	0.083
	A3	MARS-KS	0.151	0.126	0.273	0.115	0.278	0.079
	A4[1)]	RELAP5-ME	0.134	0.126	0.200	0.099	0.237	0.089
	A5	RELAP5/MOD3.3	0.126	0.107	0.202	0.099	0.249	0.072
B	B1	RELAP5/MOD3.3	0.148	0.129	0.198	0.091	0.269	0.105
	B2	MARS-KS	0.133	0.130	0.180	0.095	0.276	0.109
	B3[2)]	MARS-KS	0.109	0.132	0.165	0.093	0.204	0.092
	B4	MARS-KS	0.126	0.125	0.190	0.101	0.316	0.104
	B5	MARS-KS	0.592	0.113	0.531	0.110	0.777	0.105

Note 1) A4: Core Power was Excluded
2) B3: Hot Leg Flow Rates Were Excluded

analysis in the previous chapter, the current FFTBM application results showed very good consistency with them.

6. MAJOR FINDINGS AND LESSONS LEARNED FROM THE DSP-01 EXERCISE

In the course of the ATLAS DSP-01, intensive technical discussions on the predictions in discord with the data were made in order to segregate code deficiencies from user effects [22,23]. By analyzing the calculation spectrum and integrating common disagreements, the following major findings and lessons were learned.

6.1 Water Level Prediction in the Core and the Downcomer

Many participants agreed that the test results showed multi-dimensional effects in the core and reactor pressure vessel. For the RELAP code, the current version (MOD 3.3) predicted water levels quite well relative to the previous version (MOD 3.2), which had a tendency of over-prediction. So the RELAP MOD 3.3 should be intensively referred to in further investigations for further DSP assessment. From the discussions of the downcomer boiling effect for the prediction of the downcomer water level, its effectiveness should be further evaluated in the 100% DVI line break scenario. For a more practical approach, an interfacial drag option was recommended for a better prediction of the downcomer water level.

6.2 Loop Seal Clearing Phenomena

The loop seal clearing phenomena is very important for the behavior of water levels in the core and the downcomer. Comparisons between the test data and the calculations showed that there were quite a few discrepancies in loop seal clearing occurrence time and sequence. And there were also many discrepancies between the calculations; the reason for such different predictions was discussed and thought mainly to be due to the short period of the pressure plateau. In the case of the design code, a better prediction of the loop seal clearing would be achieved by adjusting the bubble rise velocity or the slip ratio; the effect of the downcomer bypasses to the hot legs and/or the upper head should be further investigated.

6.3 ECC Bypass

In the DVI line break scenario, the ECC bypass in the downcomer region is not considered to be important with respect to the case of the LBLOCA scenarios. In fact, there was no measured data for the ECC bypass, and, therefore, it was not possible to compare the test with the calculations.

6.4 Sensitivity Studies

Many participants conducted sensitivity studies for the steady-state and transient behavior. For the steady-state behavior, the primary fluid temperatures were adjusted by modification of the downcomer bypass flowrate (KEPRI) or speed control of the RCPs (KOPEC).

For transient behavior, many more sensitivity studies were conducted. The break flow behavior according to the variations of discharge coefficient in the critical flow models (KEPRI, KOPEC and EN2T) and the K-factor in break line (KOPEC) were investigated. The downcomer modeling with multi-D component of the MARS was investigated (KAERI), but the result was nearly the same as the base case. Many more sub-volumes for the cross-over leg and the level tracking model for those sub-volumes were adopted; the results showed a partially improved prediction for the loop seal clearing (KNF). With a higher interfacial heat transfer coefficient in the downcomer from the time of the pump safety injection, no significant improvement in the loop seal clearing prediction was observed (KNF). The initial PCT at loop seal clearing could be captured by implementing the CCFL model for the fuel alignment plate (EN2T).

6.5 User Effect

In the DSP-01 assessment, there must be user effects on the calculations. But such a user effect was not evaluated in these DSP-01 calculations. It is recommended that such an effect should be considered in the DSP-02 assessment.

7. CONCLUSIONS

The present ATLAS DSP-01 exercise was the first-ever domestic cooperative activity in which many nuclear institutions in the academic, industrial and research fields made a unified code assessment effort under a tie-up environment. It gave an opportunity for the participants to utilize the ATLAS integral effect data for their purposes and to share their individual code experiences. Ten calculations were finally performed and two best-estimate safety analysis codes were used: MARS-KS and RELAP5/MOD3.3 series.

Most calculations qualitatively succeeded in reproducing typical transient behavior during a DVI line break accident, including the primary pressure depressurization, the primary pressure plateau, the MSSV opening, the loop seal clearing, the core water level depression, and the break flow. However, there was much quantitative disagreement in predicting the PCT excursion, the degree of water level depression and the timing of the loop seal clearing. It was concluded that more attention was necessary for the water level predictions in the core and downcomer to achieve greater agreement. The multi-dimensional aspect (observed in the reactor pressure vessel) was also suspected to be the causes of this disagreement. The downcomer boiling, in particular, seemed notto have been neglected in the 100%

DVI line break accident and needs further investigation.

The prediction of the loop seal clearing was unsatisfactory. A clear and sudden occurrence of loop seal clearing was not well predicted by most calculations. The bubble rise velocity and the core bypass flow would affect this disagreement. The predicted break flow rates showed a relatively narrower scattering around the data than expected. This was because most users adjusted their break modeling based on the data.

In addition, significant user effects were observed. Calculations by less experienced users overshadowed an objective assessment of models and correlations of the codes. Nonetheless, the code deficiencies and the user effects could be segregated by the great contribution of experienced users.

A quantification of the code accuracy (based on the FFTBM) was performed with the submitted calculations. By comparing them with the qualitative comparison analysis for the submitted calculations, the present FFTBM application results showed very good consistency with these calculations; it was found that the FFTMB will be a promising and powerful automated code assessment program (ACAP).

Based on the successful and fruitful operation of the ATLAS DSP-01 exercise, the second DSP (DSP-02) program was launched focusing on a cold leg SBLOCA in the middle of 2010. As for the more productive DSP-02 program, more intensive efforts on assessments regarding the technical issues derived from the DSP-01 exercise will be pursued by the operating agency and participants.

ACKNOWLEDGEMENTS

The authors are grateful to the Ministry of Education, Science and Technology (MEST) of Korea for its financial support for this project and to the Korea Institute of Nuclear Safety (KINS) for coordination, support and analysis work.

NOMENCLATURE

AA	Average amplitude
ACAP	Automated code assessment program
AE	Architecture engineer
ASME	American society of mechanical engineers
APR1400	Advanced power reactor 1400 MWe
ATLAS	Advanced Thermal-hydraulic test Loop for Accident Simulation
CAMP	Code Assessment and Maintenance Program
CCFL	Counter-current flow limit
Cd	Discharge coefficient
CL	Cold leg
CLI	Cold leg injection
COBRA-TF	Coolant boiling in rod arrays code (two-fluid)
CS	Containment simulator
CSNI	NEA committee on the safety of nuclear installation
D	Dimensional
DC	Downcomer
DSP	Domestic standard problem
DVI	Direct vessel injection
E&C	Engineering and construction
ECC	Emergency core cooling
EN2T	Environment & Energy Technology, Inc.
f	Frequency
FCV	Flow control valve
FDIR	Facility description and instrumentation report
FFT	Fast Fourier transform
FFTBM	Fast Fourier transform based method
FLB	Feed line break
HL	Hot leg
HTC	Heat transfer coefficient
IAEA	International Atomic Energy Agency
ID	Identification
IL	Intermediate leg
ISP	International standard problem
JAEA	Japan Atomic Energy Agency
KAERI	Korea Atomic Energy Research Institute
KAIST	Korea Advanced Institute of Science and Technology
KEPCO	Korea Electric Power Corporation
KEPRI	Korea Electric Power Research Institute
KINS	Korea Institute of Nuclear Safety
KNF	Korea Nuclear Fuel, Ltd. (since Aug. 2010, named KEPCO NF)
KOPEC	Korea Power Engineering Company, Inc. (since July 2010, named KEPCO E&C)
LBLOCA	Large break loss of coolant accident
LC	Load cell
LP	Lower plenum
LPP	Low pressurizer pressure trip
LSTF	Large Scale Test Facility
LT	Level transmitter
LUDP	Low upper downcomer pressure trip
MARS	Multi-dimensional analysis of reactor safety
MF	Main feedwater
MS	Main steam
MSIV	Main steam isolation valve
MSSV	Main steam safety valve
MUG	MARS user group
N	Number of sample values
NEA	Nuclear energy agency
NETEC	Nuclear Engineering & Technology Institute
NF	Nuclear fuel
OPR1000	Optimized power reactor 1000 MWe
PCT	Peak cladding temperature
PIRT	Phenomena identification and ranking table
PT	Pressure transmitter
PWR	Pressurized water reactor
PZR	Pressurizer
QV	Volume flowmeter
RCP	Reactor coolant pump

RCS	Reactor coolant system
RELAP	Reactor excursion and leak analysis program
RHR	Residual hear removal
RPV	Reactor pressure vessel
RV	Reactor vessel
RWT	Refueling water storage tank
SBLOCA	Small break loss of coolant accident
SD	Steam dome or system design
SDD	System Design & Development, Inc.
SGSD	Steam generator steam dome
SGSDDC	Steam generator (between) steam dome (and) downcomer
SGTR	Steam generator tube rupture
SIP	Safety injection pump
SIT	Safety injection tank
SLB	Steam line break
SNU	Seoul National University
SPE	Standard problem exercise
TC	Thermocouple
T_d	Time frame selection
TF	Fluid temperature
WF	Weighted frequency
w_f	Weighting factor

Subscripts

cut	cut-off
exp	experiment
max	maximum
norm	normalized
s	sample
saf	safety (relevance)
tot	total
var	variable analyzed

REFERENCES

[1] W. P. Baek, C.-H. Song, B. J. Yun, T. S. Kwon, S. K. Moon and S. J. Lee, "KAERI Integral Effect Test Program and the ATLAS Design," *Nucl. Technol*., 152, 183 (2005).

[2] K. Y. Choi et al, "Simulation Capability of the ATLAS Facility for Major Design-Basis Accidents," *Nuclear Technology*, 156, 256 (2006).

[3] W. P. Baek and Y. S. Kim, "Accident Simulation ATLAS for APWRs," *Nuclear Engineering International*, 53, 21 (2008).

[4] Y. S. Kim et al, "Commissioning of the ATLAS Thermal-Hydraulic Integral Test Facility," *Annals of Nuclear Energy*, 35, 1791 (2008).

[5] K. Y. Choi et al., "Experimental Simulation of a Direct Vessel Injection Line Break of the APR1400 with the ATLAS," *Nuclear Engineering and Technology*, 41, 655 (2009).

[6] K.Y. Choi, et al., "Comparison Report of Open Calculations for ATLAS Domestic Standard Problem (DSP-01)," KAERI/TR-4073/2010, Korea Atomic Energy Research Institute (2010).

[7] K. Y. Choi, et al., "Integral Behavior of the ATLAS Facility for a 3-inch Small Break Loss of Coolant Accident," *Nuclear Engineering and Technology*, 40, 199 (2008).

[8] W. P. Baek et al., "LBLOCA and DVI Line Break Tests with the ATLAS Integral Facility," *Nuclear Engineering and Technology*, 41, 775 (2009).

[9] S. Cho et al., "Core Thermal Hydraulic Behavior During the Reflood Phase of Cold-leg LBLOCA Experiments using the ATLAS Test Facility," *Nuclear Engineering and Technology*, 41, 1263 (2009).

[10] H. S. Park et al., "An Integral Effect Test on the LBLOCA Reflood Phenomena for the APR1400 using the ATLAS under a Best-Estimate Condition," J. of Nuclear Science and Technology, 46, 1059 (2009).

[11] K.Y. Choi et al., "Double-Ended Break Test of an 8.5 inch Direct Vessel Injection Line Using the ATLAS," KAERI/TR-3990/2010, Korea Atomic Energy Research Institute (2010).

[12] K. H. Kang, et al, "ATLAS Facility and Instrumentation Description Report," KARE/TR-3779/2009, Korea Atomic Energy Research Institute (2009).

[13] The American Society of Mechanical Engineers, "Test Uncertainty," ASME PTC 19.1-1998 (1998).

[14] B. J. Yun et al., "Development of an Average Bidirectional Flow Tube for a Measurement of the Single and Two Phase Flow," The 11th International Topical Meeting on Nuclear Reactor Thermal-Hydraulics (NURETH-11), Avignon, France, October 2 ~ 6 (2005).

[15] Ambrosini W., Bovalini R., D'Auria F., "Evaluation of Accuracy of Thermal Hydraulic Code Calculations", *J. Energia Nucleare*, Vol. 2, (1990).

[16] D'Auria, F., Leonardi, M., Pochard, R., "Methodology for the Evaluation of Thermal Hydraulic Codes Accuracy," *Proc. Int. Conf. on New trends in Nuclear System Thermohydraulics*, Pisa, 467–477 (1994).

[17] Robert F. Kunz, Gerald F. Kasmala, John H. Mahaffy, Christopher J. Murray, "On the Automated Assessment of Nuclear Reactor Systems Code Accuracy," *Nuclear Engineering and Design*, Vol. 211, Issues 2-3, 245-272, (2002).

[18] Andrej Prosek, Francesco D'Auria, David J. Richards, Borut Mavko, "Quantitative Assessment of Thermal-Hydraulic Codes Used for Heavy Water Reactor Calculations," Nuclear Engineering and Design, Vol. 236, Issue 3, 295-308, (2006).

[19] D'Auria, F., Mazzini, M., Oriolo, F., Paci, S., "Comparison Report of the OECD/CSNI International Standard Problem 21 (Piper-one experiment PO-SB-7)," *CSNI Report No. 162*, (1989).

[20] A. Prosek, F. D'Auria, B. Mavko, "Review of Quantitative Accuracy Assessments with Fast Fourier Transform Based Method (FFTBM)," *Nuclear Engineering and Design*, 217, 179-206, (2002).

[21] B.D. Chung et al., "Phenomena Identification and Ranking Tabulation for APR1400 Direct Vessel Injection Line Break," *NURETH-10*, Seoul, Korea, October 5-9, (2003).

[22] KAERI ATLAS Team, "Meeting minutes of the 4th Progress Review Meeting of the DSP-01," Muju Ilsung-Condo, (in Korean), 2010.2.25. (2010)

[23] KAERI ATLAS Team, "Meeting minutes of the ATLAS DSP-01 Workshop," Daejon INTEC, (in Korean), 2010.4.29. (2010)